Available online at www.sciencedirect.com
ScienceDirect
Ceramics International 36 (2010) 15–21
CERAMICS INTERNATIONAL
www.elsevier.com/locate/ceramint

# Effect of α and γ polymorphs of alumina on the preparation of $MgAl_2O_4$-spinel-containing refractory cements

Araceli Elisabet Lavat *, María Cristina Grasselli, Eugenia Giuliodori Lovecchio

*Dpto. Ingeniería Química, Facultad de Ingeniería, Universidad Nacional del Centro de la Provincia de Buenos Aires, Av. del Valle 5737, B7400JWI Olavarría, Argentina*

Received 2 January 2009; received in revised form 6 April 2009; accepted 5 June 2009
Available online 10 July 2009

**Abstract**

The use of aluminous refractory materials containing $MgAl_2O_4$-spinel has led to a major breakthrough in the service life of refractory coatings applied in the industries and in the quality of the products.

Many researches have been conducted to improve the synthetic procedures in order to reduce the production cost of these materials. In this way, refractory cements involving in situ generated spinel phase have been obtained from mixtures of active alumina and dolomites. Other investigations have demonstrated that γ alumina is advantageous in comparison with the α polymorph in the synthesis and sintering properties of pure $MgAl_2O_4$-spinel.

In this article, the performance of both polymorphs of alumina, used as raw materials in the preparation of the refractory cements, along with dolomite proceeding from Olavarría, in the centre of Buenos Aires Province (Argentine), is compared.

The thermal and structural changes which take place during the firing of the batches up to 1450 °C were studied by the combination of diffractometric and infrared spectroscopy data, at the most remarkable reaction steps.

According to these results, the study of phase changes within the investigated thermal range allowed to establish the main differences in the composition of both mixtures in each firing step. Independently of the type of alumina used, a mixed phase product consisting of spinel, as a major phase, accompanied by $CaAl_2O_4$ (CA) and $CaAl_4O_7$ ($CA_2$), as secondary phases, was obtained. In addition, it was found that the formation of these phases at lower temperature is favoured by γ-$Al_2O_3$.


*Keywords:* A. Calcination; B. Spectroscopy; B. X-ray methods; Spinel-containing refractory

## 1. Introduction

The refractory properties of high alumina cements can be improved substantially when MgO is incorporated to the cement clinker replacing CaO without deleterious effect on the mechanical strength [1]. This is due to the formation of $MgAl_2O_4$-spinel in the final product. $MgAl_2O_4$-spinel is very attractive as refractory material in heavy industries because of its high melting point, low thermal expansion, considerable hardness, high resistance to chemical attack, favourable chemical stability, and good thermal spalling [2].

Spinel cements, which are aluminous cements containing between 6% and 13% of MgO, show increased thermo mechanical strength and minimal slag attack due to the $MgAl_2O_4$-spinel content [1,3]. Based on their properties these materials are being used for lining by glass, cement and siderurgy industries. As regards the latter, their utilization in casting ladles represents an outstanding improvement, not only in ladle service life but also in steel production quality.

On the other hand, $MgAl_2O_4$-spinel refractories, mainly used for cement rotary kilns, are possible alternative chromium-free refractories for secondary steel making in order to protect the environment [4].

Due to the practical considerations mentioned above, the synthesis of $MgAl_2O_4$-spinel refractories has attracted considerable attention. These materials are usually prepared by sintering from high alumina cement and synthetic $MgAl_2O_4$-spinel. However, at present, the cost of the sintered and electrofused spinels has limited their applications. Consequently, in view of the unreplaceable character of such

* Corresponding author.
*E-mail address:* alavat@fio.unicen.edu.ar (A.E. Lavat).

0272-8842/$36.00 
doi:10.1016/j.ceramint.2009.06.015

Table 1
Chemical composition of raw materials (in oxides, wt%). L.I., loss on ignition.

| Raw materials | $SiO_2$ (wt%) | $Al_2O_3$ (wt%) | $Fe_2O_3$ (wt%) | $TiO_2$ (wt%) | $P_2O_3$ (wt%) | MnO (wt%) | CaO (wt%) | MgO (wt%) | $Na_2O$ (wt%) | $K_2O$ (wt%) | $SO_3$ (wt%) | L.I. (wt%) | $d$ (μm) | $S$ ($m^2/g$) |
|---|---|---|---|---|---|---|---|---|---|---|---|---|---|---|
| Dolomite | 6.56 | 1.47 | 1.63 | 0.11 | 0.03 | 0.08 | 29.60 | 17.83 | <0.01 | 0.43 | <0.01 | 42.07 | 24.27 | 2.4 |
| α-$Al_2O_3$ | 0.02 | 99.50 | 0.02 | – | – | – | – | – | 0.30 | – | – | 0.11 | 71.60 | 8 |
| γ-$Al_2O_3$ | 0.02 | 99.17 | 0.03 | – | – | – | – | – | 0.46 | – | – | 0.15 | 9.82 | 55.98 |

materials in the industry it is necessary a greater development focussing on the alternative routes of synthesis of this kind of refractories.

The preparation of calcium aluminate cements containing $MgAl_2O_4$-spinel using appropriate mixtures of active alumina and dolomite from Spain and Egypt has already been reported [1,3]. On the other hand, it has recently been described a similar way of synthesis involving in situ generated spinel phase by using a dolomitic raw material from Olavarría District, in the centre of Buenos Aires Province [5].

Additionally, the effect of using different polymorphs of alumina as raw materials has been considered in many studies. Zhang and Li have carried out the synthesis of the refractories by conventional solid state reaction by mixing α-$Al_2O_3$–MgO, γ-$Al_2O_3$–MgO and ρ-$Al_2O_3$–MgO, and firing them at high temperature [6]. According to these results, γ-$Al_2O_3$, which belongs to the same crystal type with $MgAl_2O_4$, is more advantageous in the synthesis and sintering of pure spinel compared to α-$Al_2O_3$. The same conclusion was obtained by Domanski et al, who obtained the cements by a mechano-chemical procedure, grinding at room temperature mixes of MgO–boehmite, α-$Al_2O_3$–MgO and γ-$Al_2O_3$–MgO [2].

Considering that the most important dolomite mineral resources in Argentine are located in Olavarría District, and in order to advance in the feasibility of application of these potentially useful raw materials to prepare refractory cements, our investigation has been extended to the preparation of $MgAl_2O_4$-spinel-containing refractory cements using the α and γ polymorphs of alumina, commercially available.

In the present study, the in situ generation of $MgAl_2O_4$ (MA) from both polymorphs of alumina, is analyzed in order to establish the most adequate conditions for the solid state reaction with local dolomite. The behaviour of the different batches submitted to firing up to 1450 °C was evaluated by using the combination of spectroscopic FTIR technique and XRD analysis. The characterization of the phases obtained in each thermal step is discussed according to the thermochemical and structural changes which take place during the processes.

## 2. Experimental procedure

### 2.1. Materials characterization

Starting materials: the dolomitic raw materials employed were supplied by Polysan S.A. company (Polysan M.R., Sierras Bayas, Buenos Aires, Argentine). Available $Al_2O_3$ (BDH No. 27082) was used as a source of α-alumina. Meanwhile, γ-$Al_2O_3$ was obtained by thermal decomposition of commercial gibbsite ($Al(OH)_3$, 99%, ALCOA C-30) following a reported procedure [2]. The purity of the resulting oxide was confirmed prior to its use in the preparation of the batches.

Sieved dolomite fraction ≤125 μm was characterized from its chemical, mineralogical and grain size properties.

Particle size distribution was established by laser diffraction method in isopropyl alcohol dampened suspensions using the Malvern Matersizer-S. The surface area was determined by the BET method through the $N_2$ adsorption technique at 77 K, using a Quantachrome Nova 1200e pore size and surface area analyzer.

Chemical composition was determined by X-ray fluorescence wavelength dispersive technique in the Institute of Mineral Technology (Intemin Segemar, Buenos Aires). The fusion with lithium tetraborate was applied as preparation sample method. Reference certificated materials were used for calibration.

The chemical composition, mean particle size "*d*" and specific surface area "*S*" results of samples are given in Table 1.

Finely ground polycrystalline samples were mineralogical analyzed by FTIR vibrational spectroscopy and X-ray diffraction.

The XRD measurements were carried out with a Philips PW 3710 diffractometer with graphite monochromated Cu Kα radiation. Phase identification analysis was carried out by comparing the respective powder X-ray diffraction patterns with standard database stated by JCPDF. Table 2 shows the PDF records for every material under study together with the formula, name, symbol and main reflections used in this work.

Table 2
Nomenclature, PDF no., and principal diffraction lines of the phases under analysis.

| PDF no. | Formula, name | Symbol | $d$ (Å) |
|---|---|---|---|
| 42-1468 | $Al_2O_3$, α-$Al_2O_3$, α-alumina | αA | 2.0850 |
| 21-1096 | β$NaAl_{11}O_{17}$, β-$Al_2O_3$, β-alumina | βA | 11.300 |
| 29-0063 | γ-$Al_2O_3$, | γA | 1.4000 |
| 33-1161 | $SiO_2$, quartz | Q | 3.3420 |
| 36-0426 | $CaMg(CO_3)_2$, dolomite | D | 2.8880 |
| 05-0586 | $CaCO_3$, calcite | C | 3.0350 |
| 37-1497 | CaO, lime | CaO | 2.4058 |
| 44-1481 | $Ca(OH)_2$, portlandite | CH | 2.6270 |
| 04-0829 | MgO, periclase | M | 2.1060 |
| 21-1152 | $MgAl_2O_4$, spinel | MA | 2.4370 |
| 34-0440 | $CaAl_2O_4$ | CA | 2.9700 |
| 23-1037 | $CaAl_4O_7$ | $CA_2$ | 3.5000; 4.4400 |
| 38-0470 | $CaAl_{12}O_{19}$, hibonite | $CA_6$ | 2.4780; 2.0090 |
| 09-0413 | $Ca_{12}Al_{14}O_{33}$, mayenite | $C_{12}A_7$ | 2.6800; 2.1890 |
| 35-0755 | $Ca_2Al_2SiO_7$ gehlenite | $C_2AS$ | 2.8446; 1.7542 |
| 21-0540 | $Mg(Al,Fe)_2O_4$ | MAF | 2.4700 |
| 32-0168 | $CaFe_2O_4$ | FC | 2.6680; 1.8320 |

The FTIR spectra were measured using a Nicolet-Magna 550 instrument, with CsI optics applying the KBr ''pellets'' technique. Spectra interpretation was based on published data [7–13] and FTIR spectra of Minerals Library software.

### 2.2. Samples preparation

Two batches of cement samples consisting of appropriate amount of each alumina polymorph and dolomite, labelled DαA and DγA, were studied. These are referred to as the materials prepared from αA and γA, respectively. Considering the $Al_2O_3$–MgO–CaO ternary system phase diagram [14,15] as well as the chemical composition of dolomite, detailed in Table 1, mixtures of $Al_2O_3$ and 51% dolomite were prepared in order to obtain two batches of cement samples bearing the maximum spinel phase feasible and 40–45 wt% of $CaAl_2O_4$ (CA), as main hydraulic phases.

The mixtures were dry-homogenized. Half of the mixtures were submitted to conventional ceramic procedure by solid state reaction at high temperatures with intermediate grindings. The rest was pressed at approx 200 MPa and the ''pellets'' were thermally treated simultaneously with the powdered sample preparation. Although both alternatives were carried out for purposes of comparison, the latter procedure is more feasible at an industrial level. Firing was carried out in a muffle furnace under atmospheric condition.

In order to state phase changes occurring during firing as well as the optimum temperature to obtain the main components of the desired cement, samples at different firing temperatures were taken out off the furnace. According to this, the highest temperature of the firing schedule was 1450 °C.

To stabilize the ceramic bond, the materials were kept at intermediate temperatures for 1 h and at the highest temperature for several hours. The samples treated at the various temperatures, in the thermal interval, were mineralogical characterized applying the same methodology as described for raw materials.

## 3. Results and discussion

### 3.1. Characterization of raw materials

According to the chemical analysis of raw materials given in Table 1, it may be seen that the major impurities of the dolomitic source under study are $SiO_2$, $Fe_2O_3$ and $K_2O$, bearing a higher $SiO_2$ content than those used by other researchers which are around 0.02–0.5 wt% [1,3]. Meanwhile, the mean size particle of the dolomitic mineral is 24.27 μm and surface area is 2.4 $m^2/g$.

On the other hand the chemical compositions of both $Al_2O_3$ polymorphs are similar showing higher purities than the aluminous source used in other experiments [6] over 99.10% pure, and similar weight loss on ignition. Nevertheless, the particle mean size and specific surface of both polymorphs are markedly different. An enhancement in the reactivity of γ-$Al_2O_3$ is expected since *S* value is markedly higher than that of α-$Al_2O_3$ polymorph.

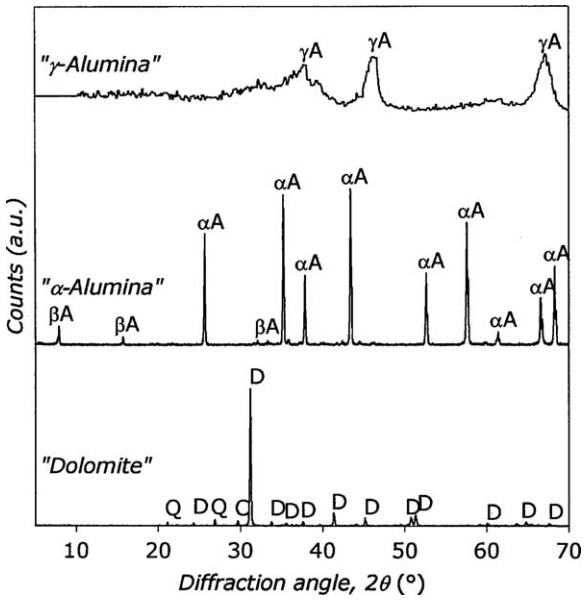


Fig. 1. Minerals characterization of raw materials, XRD patterns.

Fig. 1 shows the XRD pattern of both alumina raw materials. In addition, the PDF records for raw materials, as well as the files belonging to the rest of the phases under analysis, are detailed in Table 2, as already stated. Based on this analysis, it is concluded that the dolomite sample also contains calcite (C) and quartz (Q) but in a lesser extent. In the case of the calcined alumina a major content of α-$Al_2O_3$ is observed whereas β-$Al_2O_3$ is low. These results agree with the chemical composition reported in the previous researches.

The FTIR spectra of the raw materials can be seen in Fig. 2. Dolomite shows its overall bands, among which the diagnostic ones at 1443, 882 and 728 $cm^{-1}$ belonging to $CO_3^{2-}$ anion are present [6].

Calcite bands are not seen because they are located at similar frequencies as dolomite ones (1428, 878 and 714 $cm^{-1}$) and therefore overlapped with the bands of this predominant mineral.

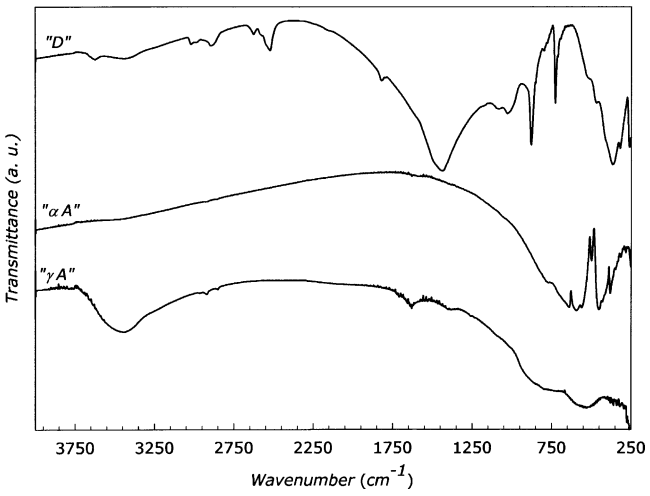


Fig. 2. FTIR spectra of starting materials.

Nevertheless, quartz, being a minor constituent, can clearly be identified by the bands located at 1144 and 1085 $cm^{-1}$, which are attributed to $SiO_4$ group vibrations, as these bands are conveniently separated.

Alumina is recognized by a series of bands located in the region 250–750 $cm^{-1}$, belonging to the "condensed" $AlO_6$ octahedra, which constitute the building units in α-$Al_2O_3$ structure. Among them, the two strong absorptions at 650 and 600 $cm^{-1}$, considered the diagnostic ones for this material, are clearly noticeable [12].

As it may also be seen in Fig. 2, the FTIR spectrum of γ-$Al_2O_3$, shows poorly resolved bands due to the low crystallinity of this material. The main absorptions lying at 500–680 and 700–800 $cm^{-1}$, are assigned to the $AlO_6$ "condensed" octahedra and to $AlO_4$ "isolated" tetrahedra which are the building blocks forming the structure of this type of alumina, respectively. The weak bands centred in 1620 and 3470 $cm^{-1}$, located in the mid- and high-energy region of the spectra are related to deformational and asymmetric stretching of H–OH bonds, respectively. The presence of these bands in the spectrum of γ-$Al_2O_3$ has already been attributed to the remnant hydrogen of hydrated alumina-gibbsite, employed as source of $Al_2O_3$ [13].

### 3.2. Evolution of the phases on heating by X-ray diffraction

For the detailed analysis of the phase changes during the preparation of both cements, in every thermal step, the relative intensity of the characteristic peaks of each crystalline compound expected to appear was measured, within the temperature range 800–1450 °C. The instrumental conditions were maintained constant in order to obtain the comparison of the same XRD characteristic lines by using "batch program" analysis in PC-APD software (version 3.6). The typical reflections selected to carry out the analysis are detailed in Table 2.

The XRD patterns belonging to the different heating temperatures selected to represent the phase evolution upon calcinations, for the batches labeled DαA and DγA are shown in Figs. 3 and 4.

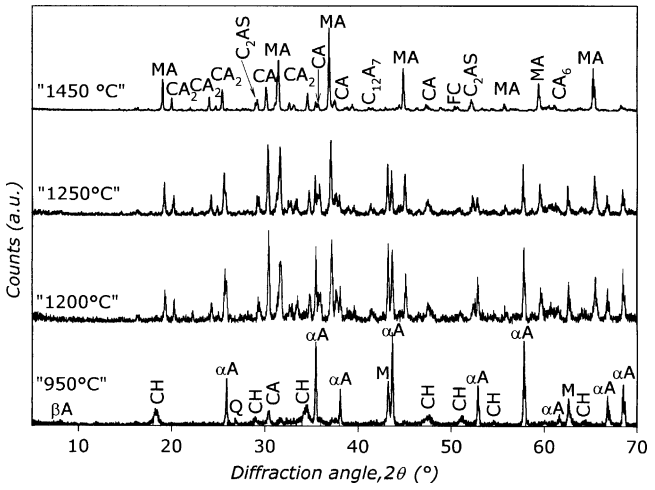


Fig. 3. XRD patterns of sample DαA at different firing temperatures.

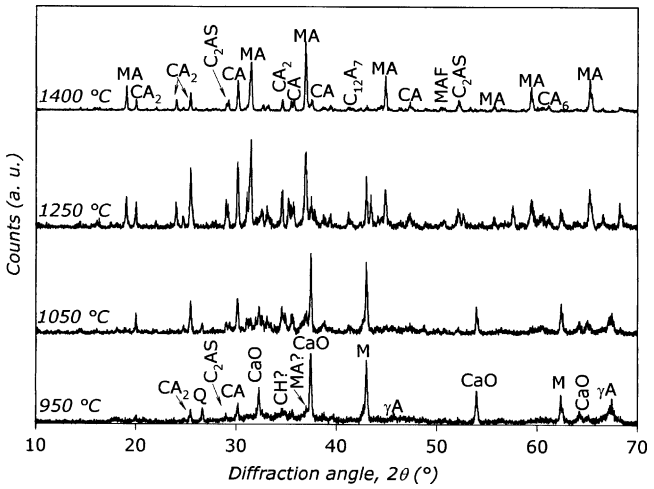


Fig. 4. XRD patterns of sample DγA at different firing temperatures.

For more detailed information, the XRD main diffraction intensities of every component detected in the patterns is plotted against temperature, as can be seen in Fig. 5a and b. When there is an overlap of the main peaks for two phases, the second reflection reported in Table 2 was also used. Based on this, the evolution of phases during firing was estimated.

No dolomite is detected at 950 °C in any of the two samples, DαA or DγA. At the same time, in the case of sample DαA, the main peaks associated with α-$Al_2O_3$ are still present. The new phases resulting from the thermal decomposition of D, and by reaction with $Al_2O_3$, as M, CH, Ca-aluminates and free CaO (only in the case of DγA) were detected. The MgO formed remains stable but CaO is mainly present as CH-portlandite and CA, in sample DαA. Portlandite is formed as a result of the high reactivity of CaO with atmospheric humidity and the remaining CaO combines with α-$Al_2O_3$ rendering CA. In the case of sample DγA, Ca aluminates CA, $CA_2$, $C_{12}A_7$ and free CaO are clearly observed at this temperature.

Simultaneously, the presence of the silico-aluminate $C_2AS$ is attributed to the solid state reaction involving $SiO_2$ from Q, present in dolomitic raw material. The early formation of the in situ spinel MA is supported by the appearance of its main diffraction as a weak signal, which partially overlaps with the one belonging to CaO (see Table 2). The diffraction lines of CH are more clearly observed in the pattern of DαA surely because in this case the only aluminate phase present is CA, whereas in the case of DγA some peaks are superimposed with those belonging to CA, $CA_2$, and $C_{12}A_7$. In spite of this, it was possible to accurately confirm the presence of CH by the FTIR spectra, as will be seen further in the text.

At 1050 °C, in DγA, the peaks belonging to the spinel MA are clearly distinguishable from CaO. At the same time, the formation of $CA_6$ could be ascertained.

In the batch DαA the apparitions of MA, $CA_2$, $CA_6$, $C_{12}A_7$ and $C_2AS$ occur at higher temperature (≈1150 °C) than in DγA. This fact is explainable by the structural correlation between γA and the reaction products [2,6].

When the temperature reaches 1150 °C, in both batches DαA and DγA, Q signals disappear. On the other hand, the

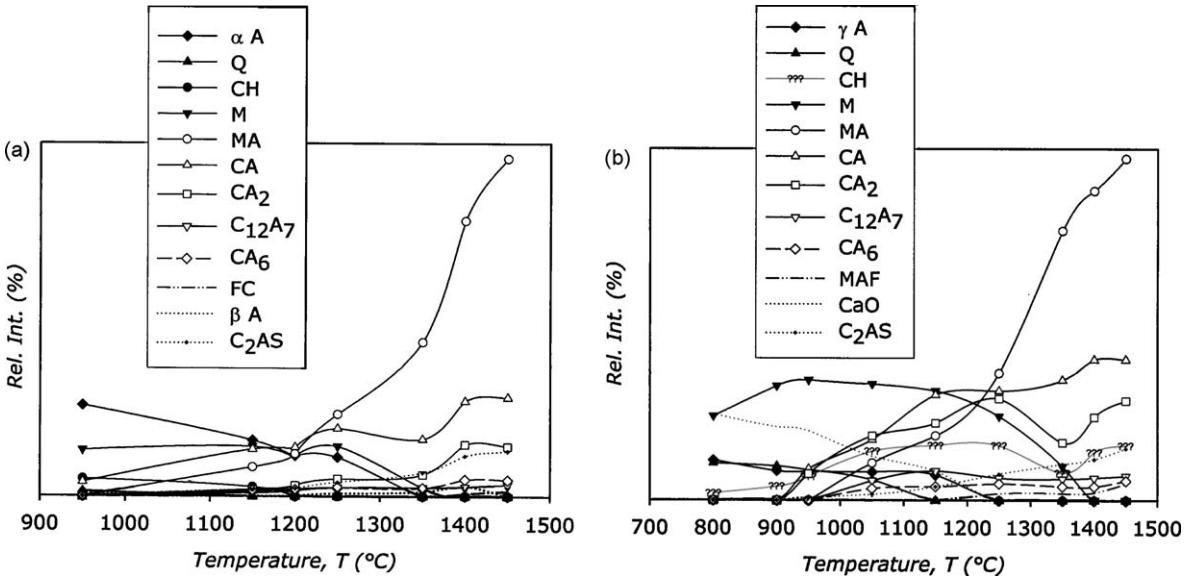


Fig. 5. Changes in the composition of phases by XRD analysis in the thermal range 950–1450 °C for each specimen: (a) DαA and (b) DγA.

amount of M is not diminished as could be expected if the spinel MA is formed by reaction of MgO. This evidence suggests that probably some dolomite, not detected by XRD, was still present at 950 °C. As will be seen later, the presence of remnant dolomite at this temperature could be confirmed by FTIR due to the higher sensibility of this technique.

Over 1250 °C, MA becomes the major component, in DαA as well as in DγA samples. Simultaneously, in the case of DγA, the oxide precursors γA and CaO precursors disappeared; and at the same time a small amount of MAF is observed. The latter solid is formed from γA and $Fe_2O_3$, consistent with the low proportion of iron oxide, determined by X-ray fluorescence, in the dolomitic mineral (see Table 1).

During the thermal treatment of DαA, at 1350 °C, the reaction between $Fe_2O_3$ and CaO takes place giving rise to the formation of little FC. At the same time, γA is no longer present.

The MgO is not present after the thermal step at 1400 °C, for both specimens. Accordingly, the final composition of the sample prepared from γA, labeled DγA, contains: MA, CA, $CA_2$, $CA_6$, $C_{12}A_7$, $C_2AS$ and MAF. On the contrary, the thermal evolution of sample DαA persists up to 1450 °C, until the total disappearance of βA.

Finally, no vitreous components are observed in both refractory cements; spinel MA and the aluminate CA can be estimated as the main phases. On the other hand, it can be seen that the amount of silico-aluminate $C_2AS$ is not negligible. This evidence is in accordance with the relatively high content of $SiO_2$ found in local dolomite, in comparison with the amount reported for the same mineral in other countries [1,3].

### 3.3. FTIR analysis

The FTIR vibrational spectra depicted in Figs. 6 and 7 are suitable to complement XRD information in order to get a more accurate composition of phases at each thermal step during the synthesis of the refractory cements DαA and DγA. The advantage of using IR spectra is that, apart from good crystalline compounds, poorly crystallized and even amorphous materials can also be identified.

According to Figs. 6 and 7, after the thermal step at 950 °C, both specimens show a significant band located at 1428 $cm^{-1}$, assigned to $CO_3^{2-}$, characteristic of dolomite [11]. The characteristic diffraction line of D could not be detected by XRD analysis, as already discussed. Nevertheless, due to the higher sensibility of the spectroscopic technique, this band is persistent in the spectrum up to 1200 °C. This also explains the rather high values of the characteristic peaks of M, observed by XRD diffraction at 1150 °C.

At the same time, the presence of CH up to 1200 °C can be ascertained by the sharp absorption at 3643 $cm^{-1}$, assigned to O–H stretching vibration belonging to $Ca(OH)_2$, which becomes weaker as temperature increases, until it completely disappears at 1250 °C in DαA, and at 1150 °C, in the case of DγA.

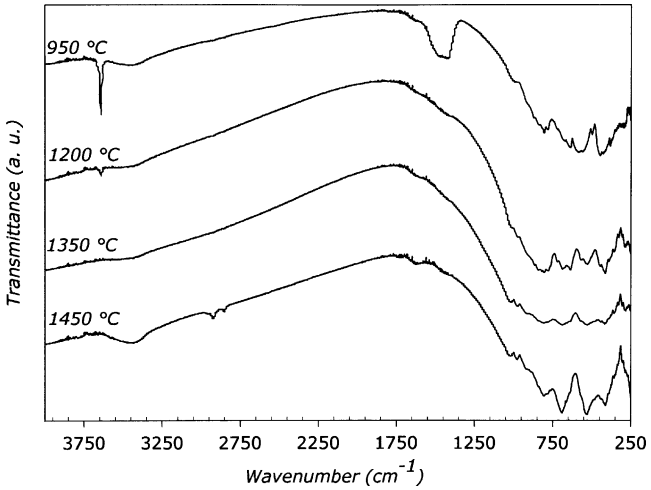


Fig. 6. FTIR spectra of DαA specimen treated in the thermal range 950–1450 °C.

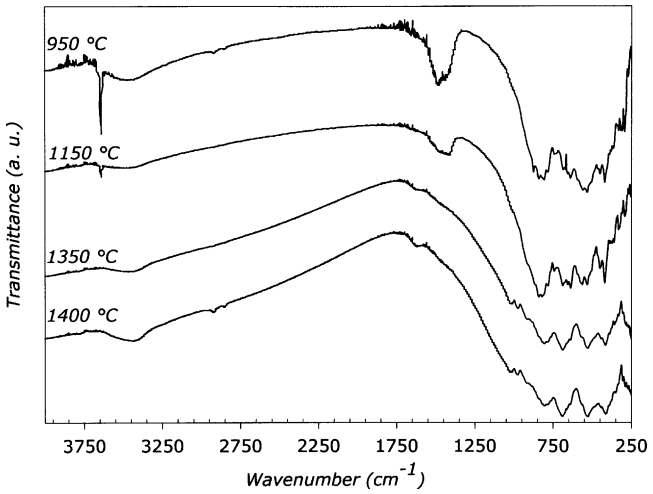


Fig. 7. FTIR spectra of DγA specimen treated in the thermal range 950–1400 °C.

The Al-phases αA, γA, CA, $CA_2$, $CA_6$, $C_{12}A_7$ and MA give rise to a rather complex spectra since the Al–O vibrations present in these oxides absorb in the same spectral region due to their bonding and coordination features. Nevertheless, the identification of the different aluminous phases by FTIR spectra was possible by comparison with the published spectra of numerous aluminates and related systems [7–13].

The spectrum of DαA treated at 950 °C, shows that the two characteristic absorptions of αA, belonging to ''condensed'' $AlO_6$ stretching vibrations, are distinguishable at 600 and 650 $cm^{-1}$. These spectral features disappear when the temperature increases due to the decrease of this mineral as the conversion progresses.

On the other hand, in the spectra of DγA at the same temperature, the absorptions observed at 750–900 $cm^{-1}$ are attributed to the stretching of ''condensed'' $AlO_4$ building units, present in CA. As temperature increases these bands become better resolved, consistent with increasingly CA that forms from γA. This result gives additional support to XRD data, according to which the complete depletion of γA was observed at 1250 °C. Conversely, the typical bands belonging to CA, also observable in sample DαA at 950 °C, are not so well resolved than in DγA. The spectral resolution markedly improves as temperature rises, at the same time as continuously αA decreases, according to XRD measurements, until its total disappearance at 1350 °C.

The spinel MA can be readily distinguished by two characteristic bands, located at 538 and 690 $cm^{-1}$, assigned to Al–O stretching arising from ''condensed'' $AlO_6$ polyhedra forming the spinel lattice [10,12]. These absorptions are clearly distinguished in the spectrum of DγA, treated at 950 °C, confirming that MA is formed ''in situ'', as already demonstrated by XRD analysis. These bands enhance their intensity and resolution accompanying the increase of MA when temperature rises.

The crystal structures of $CA_2$ and $C_{12}A_7$ aluminates, as well as CA, are formed by ''condensed'' $AlO_4$ tetrahedra. The characteristic Al–O stretching vibrations associated with these building units are located between 750 and 900 $cm^{-1}$. The counterpart of these vibrations belonging to the angular deformation modes of the same polyhedra are lying in the region at 400–500 $cm^{-1}$ [2]. In the case of $C_{12}A_7$ a typical absorption region at 3500–3700 $cm^{-1}$, related to the hydration of this aluminate, is also present due to its reactivity when the material is exposed to ambient humidity [13].

In turn, in the case of DαA, the bands associated with aluminates are not detected until the sample is treated at 1200 °C.

Regarding the bands located at 977 and 1019 $cm^{-1}$, they are attributed to Si—O—Al mixed stretching modes of the aluminosilicates moieties. These vibrations are observed, in the beginning, as a ''shoulder'' in the spectrum of sample DαA, treated at 950 °C, and subsequently its definition improves as temperature increases, as can be seen in Fig. 7. In the case of sample DγA, the same spectral signals are clearly observed from 1200 °C.

The structure of the double mixed oxide FC, observed by XRD, as a minor phase in sample DαA, give rise to vibrations which absorb at slightly lower frequencies than the ''condensed'' $AlO_4$ tetrahedra belonging to the aluminates [12]. Having in mind that this phase is formed in a small amount, their characteristic bands are surely overlapped with the aluminate signals which absorb in the same spectral region. For the same reason, the bands belonging to the ferrous-aluminate spinel MAF, are not possibly observed since its vibrations are coincident with the ones belonging to MA.

The spectral features of DγA are maintained, showing the maximum definition when the end products are formed, from 1350 °C. The same evidences are observed for DαA, from 1400 °C.

Finally, the FTIR spectra for materials departing from αA and γA are in full agreement with XRD results. Accordingly, the optimal temperatures for the refractory cement processes, using αA and γA, are 1400 and 1350 °C, respectively.

## 4. Conclusions

The polymorphism of alumina influences on the preparation route of aluminous refractory cements, which contain in situ generated $MgAl_2O_4$.

The phases formed during the synthesis of DαA and DγA cements could be well characterized, structurally and spectroscopically, by combination of XRD and FTIR techniques.

The main reactions start over 950 °C in DγA and 1150 °C, in the case of DαA; and the optimum temperature for the in situ generation of spinel phase are 1400 and 1450 °C, respectively. Consequently the formation of these phases at a lower temperature is favoured by γ-$Al_2O_3$.

In both cases, the principal co-products obtained are the hydraulic phases CA and $CA_2$. In addition to this, no vitreous phase was detected and quartz, present in the dolomitic material, forms the aluminosilicate $C_2AS$.

## Acknowledgment

This work is supported by SECAT, UNCPBA.

## References


[1] N.M.A. Khalil, S.A.S. El-Hemaly, L.G. Girgis, Aluminous cements containing magnesium aluminate spinel from Egyptian dolomite, Ceram. Int. 27 (2001) 865–873.

[2] D. Domanski, G. Urretavizcaya, F.J. Castro, F.C. Gennari, Mechanochemical synthesis of magnesium aluminate spinel power at room temperature, J. Am. Ceram. Soc. 87 (11) (2004) 2020–2024.

[3] A.H. De Aza, P. Pena, M.A. Rodríguez, R. Torrecillas, S. De Aza, New spinel-containing refractory cements, J. Eur. Ceram. Soc. 23 (2003) 737–744.

[4] K. Goto, W. Lee, The direct bond in magnesia chromite and magnesia spinel refractories, J. Am. Ceram. Soc. 9 (7) (1995) 1753–1760.

[5] A. Lavat, M.C. Grasselli, Phase evolution during preparation of spinel-containing refractoty cements, from Argentine dolomite, Adv. Technol. Mater. Mater. Proc. J. 9 (1) (2007) 103–108.

[6] Z. Zhang, N. Li, Effect of polymorphism of the synthesis of magnesium aluminate spinel, Ceram. Int. 31 (2005) 583–589.

[7] J.T. Kloprogge, H.D. Ruan, R.L. Frost, Thermal descomposition of bauxite minerals: infrared emission spectroscopy of gibbsite, boehmite and diaspore, J. Mater. Sci. 37 (2002) 1121–1129.

[8] J.M. Saniger, Al–O infrared vibrational frequencies of γ-alumina, Mater. Lett. 22 (1995) 109–113.

[9] A.M. Hofmeister, B. Wopenka, A.J. Locock, Spectroscopy and structure of hibonite, grossite, and $CaAl_2O_4$: implication for astronomical environments, Geochim. Cosmochim. Acta 68 (21) (2004) 4485–4503.

[10] S.D. Ross, Inorganic Infrared and Raman Spectra, McGraw-Hill, UK, 1972.

[11] M.J. Wilson, A Handbook of Determinative Methods in Clay Mineralogy, Blackie & Son Ltd, London, 1987.

[12] P. Tarte, Infra-red spectra of inorganic aluminates and characteristic vibrational frequencies of $AlO_4$ tetrahedra and Al $O_6$ octahedra, Spectrochim. Acta 23A (1967) 2127–2143.

[13] G. Paglia, Determination of the structure of γ-alumina using empirical and first principles calculations combined with supporting experiments, PhD Theses, Curtin University of Technology, Australia, 2004.

[14] A.C. Tas, Chemical preparation of the binary compounds in the calcia–alumina system by self-propagating combustion synthesis, J. Am. Ceram. Soc. 81 (1998) 2853–2863.

[15] A.H. De Aza, P. Pena, S. De Aza, Ternary system $Al_2O_3$–MgO–CaO: I. Primary phase field of crystalization of spinel in the subsystem $MgAl_2O_4$–$CaAl_4O_7$–CaO–MgO, J. Am. Ceram. Soc. 82 (1999) 2193–2203.